MRS Advances (2024) 9:531–536
https://doi.org/10.1557/s43580-024-00784-6

ORIGINAL PAPER

Towards the development of an electrochemical random access DNA memory (e-RADM)

Miguel A. Jimenez-Munoz[1,2] · Christopher Wood[1] · Christoph Wälti[1,2]

Received: 17 November 2023 / Accepted: 21 January 2024 / Published online: 3 April 2024

Abstract

As a result of the exponentially growing amount of information being produced, new data storage solutions are required. DNA has attracted significant attention as a potential data storage medium thanks to several intrinsic properties, such as ultrahigh physical information density with up to 2 bits per nucleotide. Current DNA-based memories rely on sequencing strategies for data recovery. However, sequencing all DNA strands for data retrieval would be very time consuming and thus result in high levels of latency. Therefore, random access strategies are required to make DNA-based data storage a viable alternative. Here, we present our first steps towards the development of a compartmentalized electrochemical random access DNA memory (e-RADM) using cascade reactions controlled by DNA nanostructures immobilized on gold microelectrode arrays which will be triggered when a specific information retrieval query is put into the system. Electrodes containing the desired information can then be identified by Square Wave Voltammetry.

Introduction

Over the last decade, the amount of data generated globally has increased exponentially and is expected to reach 1.75×10^{14} GB by 2025. Current silicon-based storage technologies, such as magnetic tapes, are struggling to keep up [1]. Therefore, new approaches to data storage using materials which offer a higher data storage density than current technologies are required. Significant efforts have been put into the integration of biomolecules with electronic devices. These biohybrid systems promise higher performance in non-volatile memory applications albeit with much lower energy requirements [2]. Examples include protein-based memristors, where proteins are the central component of the conductivity switching mechanism driven by the voltage applied [3, 4]. At the same time, DNA emerged as a promising bioelectronic alternative for next generation data storage technology owing to its Shannon capacity of 2 bits of information per nucleotide [5]. This would yield a theoretical density of 1.7×10^{19} bytes/g, enough to store all data expected to be produced by 2025. In addition, unlike most silicon-based counter parts, DNA-based memories have an exceptionally long lifetime and don't need to be regenerated frequently. Furthermore, stored information requires no power to be maintained [6]. Currently, most DNA data storage solutions exploit the actual sequence of the DNA to store information, i.e. data are encoded from binary to quaternary code, and then DNA strands are synthesized accordingly using the four natural nucleotides A, T, C and G. Data can be then retrieved by sequencing technologies and decoded back to the original format [7]. However, the requirement to sequence fully all DNA strands for retrieving a specific subset of information would imply very high levels of latency and risk the integrity of the information. Random access strategies have been developed to avoid this issue. Polymerase Chain Reaction (PCR) is currently the gold standard as specific primers can be used as the query for retrieving only the desired information. Organick *et al.* demonstrated the recovery of 200 MB of information from a theoretical 1 TB DNA memory using this approach [8]. However, as size of the DNA memory increases, the likelihood of primer cross-reactivity increases which will lead to nonspecific retrieval.

Here, we present the first stages of an electrochemical random access DNA memory (e-RADM), which utilizes DNA origami nanostructures and localized strand displacement

✉ Christoph Wälti
c.walti@leeds.ac.uk

[1] School of Electrical and Electronic Engineering, Faculty of Engineering and Physical Sciences, University of Leeds, Leeds LS2 9JT, UK

[2] Bragg Centre for Materials Research, University of Leeds, Leeds LS2 9JT, UK

reactions (SDRs) for data manipulation. Short DNA hairpins containing toeholds complementary to the sequences of adjacent hairpins are attached to a DNA origami such that cascades of SDRs can occur. When a data retrieval query is submitted in the form of a short oligonucleotide, only those hairpins with toeholds complementary to the query oligo will open, triggering a cascade reaction. Once the cascade reaction completes, the loops of the hairpins are exposed, containing the information related to the query. The hairpins are labelled with Methylene Blue (MB), and when they are immobilized on a gold electrode, the completion of the cascade reaction can be monitored by electrochemical means. Briefly, when in the hairpin is in the closed state, the MB is in close proximity to the surface thus enabling high rates of electron transfer from the surface to the MB. When the cascade completes, the end of opened hairpins is on average significantly further away from the electrode surface, thus reducing the ability of electrons from the surface to transfer to the MB. In this work, we use Square Wave Voltammetry (SWV) for the monitoring of the cascade reaction due to its proven higher sensitivity over other electrochemical methods such as Cyclic Voltammetry or Chronoamperometry, as non-faradaic currents are dismissed [9]. Therefore, the aim of this work is to develop a fully functional electrochemical device in which functionalized DNA origami structures are immobilized on a gold microelectrode array. We argue that an electrochemical data retrieval approach will help to integrate DNA-storage with existing electronic devices. Recent advances in electrochemical DNA synthesis and *in situ* sequencing further support this claim [10], opening the door of a fully integrated DNA memory without requiring external sequencing.

Here, we investigate first the opening of a single hairpin and a 2-hairpin cascade in solution, followed by the opening of hairpins immobilized on DNA nanostructures. We also demonstrate the electrochemical detection of hairpin opening using SWV as a proof of concept of the system.

Materials and methods

Opening of 20 nM of G3/Cy5:A3*/Cy3 which were annealed at a 1:1 ratio on a thermocycler (95 °C for 5 min, followed by a decrease of 1 °C min to 20 °C) and G2:A2*+G3/Cy5:A3/Cy3 (1:1) (annealed as above) was analysed in triplicates by adding 60 nM of F3 and F2, respectively. The buffer, referred as SDR buffer, used consisted of 20 mM Tris-HCl, 200 mM NaCl, and 10 mM $MgCl_2$, at pH 8. Fluorescence was recorded every 5 s for 10 min (λ_{ex} = 535 nm, λ_{em} = 680 nm). Interaction of G2–G3 in the absence of F2 was performed in a similar way, but changing the G2 concentration as described in Fig. 1e. Measurements were performed on

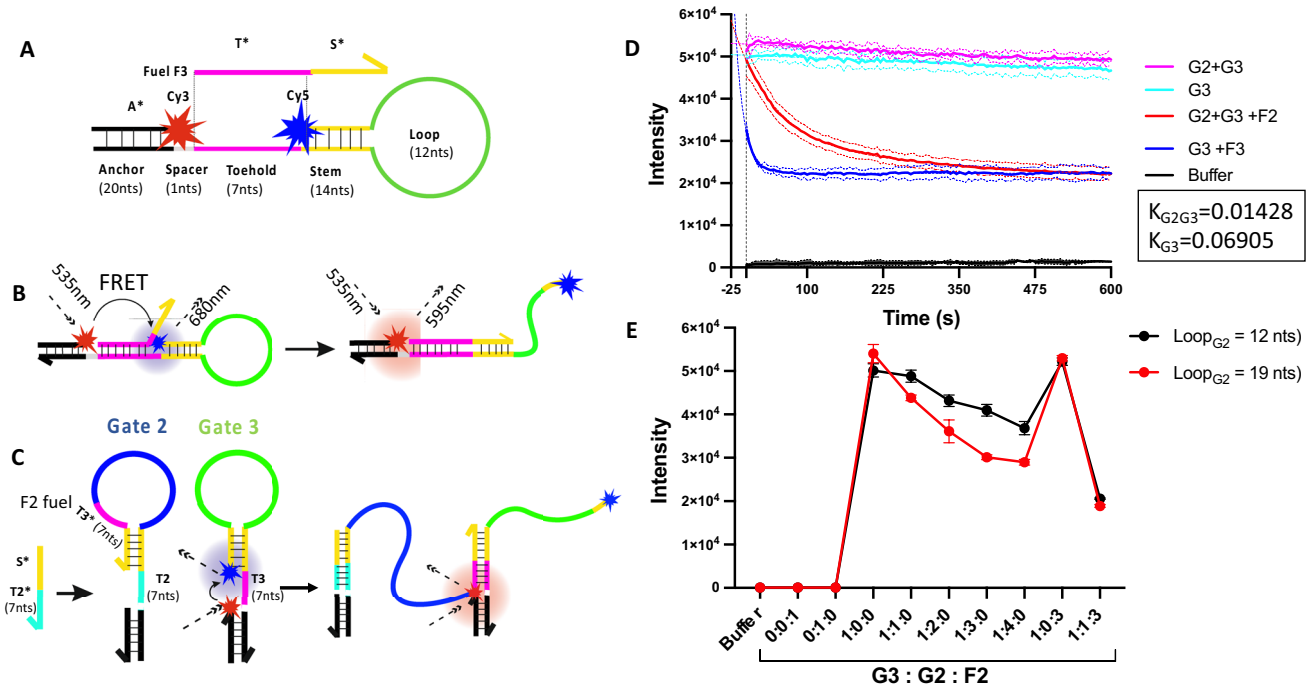

Fig. 1 **a** Schematic representation of the G3 hairpin and fuel F3. **b** Toehold-Mediated Strand Displacement (TMSD) reaction and Cy3–Cy5 FRET mechanism. **c** G2-G3 cascade reaction triggered by F2 TMSD reaction. **d** Hairpin opening kinetics of 20 nM G3 and 20 nM G2–G3 cascade triggered by 60 nM of F3 and F2, respectively. e) Analysis of 20 nM of G3 TMSD reaction triggered by G2 in the absence of F2 at different G2 concentrations and two loop lengths

a black flat 96-well plate blocked with 5% (w/v) BSA for 1h at RT.

DNA origami nanostructures were folded in a 1:10:100 molar ratio of M13mp18 scaffold:staple/extended staple:hairpin, with a 1:20 ratio of scaffold:biotinylated extended staple. The annealing was performed in SDR buffer as described for hairpin preparation. For the purification, 100 ng of Streptavidin-coated magnetic beads (New England Biolabs) were used per 5 nmol of scaffold, incubated for 30 min at RT. After washing 3x, 12 pmol of unlocker sequence was then added to release the origami structures.

For AFM imaging, 25 ng of origami was adsorbed on a mica surface by ion exchange using a 10 mM $NiCl_2$ solution, and images were recorded using peak force tapping mode in fluid with Bruker FASTSCAN-D proves.

1 nM of purified origami was used for the opening kinetics experiments of the immobilized hairpins. Fluorescence was recorded as described for free hairpins, with 2 nM final concentration of F3 or F2.

Gold microelectrode arrays were first cleaned with piranha solution (30%(v/v) H_2O_2:H_2SO_4 at a 1:3 ratio) for 5 mins. 1 µM of thiolated A3* probe in 1M KH_2PO_4 was added by drop-casting and incubated overnight at 4 °C. 1 µM of 6-mercaptohexanol on the same buffer was then added for 1 h at RT. 2 µM of G3 was annealed in SDR buffer containing 50 µM of Methylene Blue (MB). This was then added to the electrodes by drop-casting and incubated for 1 h at RT. The system was then mounted in a custom-made microfluidic chamber and connected to a BioLogic potentiostat. For Cyclic Voltammetry measurements, 9 mM of Potassium Ferro/ferricyanide sample in 0.1 M KCl was added. 3 cycles at a 100 mV/s scan rate on an overpotential range from − 0.8 to 0.8 V vs external Ag/AgCl reference electrode were recorded. Square Wave Voltammetry analysis was performed in SDR buffer. The scanning was performed over an overpotential range from − 0.1 to − 0.5 V vs external Ag/AgCl reference electrode, applying a pulse height of 25 mV, pulse width of 50 mV, and step height of 10 mV.

Data presented in this paper were analysed with GraphPad Prism (10.1.0). Diagrams were drawn using CorelDRAW (technical suite 2023).

Results

Kinetics of the toehold-mediated strand displacement (TMSD) reaction and TMSD-triggered cascade reaction

We evaluated the opening of two hairpins, referred to as Gate 2 (G2) and Gate 3 (G3). These hairpins were designed in NUPACK software [11], where secondary structures and cross-interactions were evaluated at 25 °C. G3 and G2 structures are shown in Fig. 1a, c, respectively, and their full sequences can be found in the supplementary information. G3 was labelled with Cyanine5 (Cy5) fluorochrome at the 5′-end, and paired with a Cyanine3 (Cy3)-labelled 20nts oligo complementary to its anchor tag region, referred as A3*. This allowed us to monitor the opening kinetics of the hairpin by Foster Resonance Energy Transfer (FRET). The opening of the hairpins is promoted by a TMSD reaction as indicated in Fig. 1b, in which a short, single-stranded overhang region (known as toehold) initiates the strand displacement. A short oligo, referred as fuel F3, binds to G3's toehold and invades its stem region, displacing the S* sequence. For the cascade reaction, the unzipping of G3 is triggered by G2 when it has been previously opened by a short oligonucleotide, referred as fuel F2 (Fig. 1c). The F3 sequence is contained within the loop of G2, which is only accessible when G2 has been fully opened.

The FRET signal of a 20 nM sample of G3 and G2+G3 was studied upon adding F3 and F2, respectively, to open the loops. As shown in Fig. 1d, both G3 and G2+G3 FRET signals drifted only slowly over time when no fuel is added. However, when the fuel F3 is added to the G3 sample, the FRET signal is rapidly reduced over time, reaching a plateau within 30 seconds. The G2–G3 cascade reaction is significantly slower, only reaching a plateau after 6 minutes. The data were fitted to an exponential decay equation allowing for a small linear drift, which is likely the result of DNA strands adsorbing to the microplate wells even after blocking them with BSA. The FRET signal is described as:

$$Y = Y_M - (Y_M - Y_0) \cdot e^{-K \cdot X} - Y_1 \cdot X,$$

where Y_0 starting intensity, Y_M maximum intensity, K hairpin opening rate and Y_1 slope of small drift.

The decay rate was found to be approximately 7 times slower for the cascade when compared to the opening of a single hairpin (Fig 1d).

The opening of the G2–G3 cascade was further evaluated with different G2:G3 ratios and G2 loop length, to ensure the cascade is only triggered by the fuel F2. As can be seen in Fig. 1e G3 is gradually opened as G2 concentration is increased, as well as for a longer loop. However, at a 1:1 G2:G3 ratio for the shorter loop, the FRET signal is almost identical to G3 alone, indicating suitable conditions for the cascade reaction.

Immobilization of hairpins to a flat DNA origami structure

Developing a localized cascade reaction is a crucial point for our RADM strategy. Hairpins have to be spatially separated at an adequate distances such that communication for a TMSD reaction is possible.

As a proof of concept for our immobilization method, three different hairpins, G2 and G3, as well as an additional hairpin G1, were immobilized on a flat DNA origami structure, spaced apart by 40 nm by introducing staples with an extended region complementary to the anchor tag sequence of each hairpin on those positions (Fig. 2e). Hairpins were introduced during the folding step of the origami structure at a 1:100 ratio of M13mp18 scaffold:hairpin, and origami structures were purified from free staples and hairpin using magnetic streptavidin-coated beads. Fig. 2b shows an AFM image of the DNA origami structures with immobilized hairpins which can be seen as bright spots on the DNA origami. Fig. 2c shows an individual DNA origami with the line profile across the positions where the 3 hairpins are expected to be located, and 3 peaks spaced by approximately 40 nm can be seen clearly indicating successful immobilization. Finally, Fig. 2d shows the line profile of an origami structure functionalized just with G3 hairpin, demonstrating that the hairpins are binding specifically to their intended positions.

Preliminary opening kinetics of hairpins on origami structure

Following the successful immobilization of the hairpins on the origami, the opening of G3 and G2-G3 was investigated. The extended staple at the G3 position contained a Cy3 label and the FRET signal 1 nM G3-functionalized origami was measured over time. The signal drifted only negligibly over time, but decreased rapidly when 2 nM final concentration of fuel F3 was added, with an opening rate of one order of magnitude lower than free G3 (Fig. 3a).

The G2–G3 cascade with the hairpins immobilized 40 nm apart on the DNA origami. However, the FRET signal remained constant over time in both the absence and presence of F2, indicating that the hairpins were not interacting with each other (Fig. 3b). This was to be expected and is consistent with the fact that the length of the hairpin, even in the open state (~30 nm), is too short to bridge the distance of 40 nm. Future iterations will consider the effect of the separation of G2–G3 to determine the optimal distance for the cascade to be triggered.

We note that these results are preliminary and the system needs to be further optimized. While the AFM images show the successful immobilization of the hairpins, we cannot yet guarantee that all hairpins have been from solution, and further analysis is required.

Electrochemical monitoring of G3 hairpin opening

The opening of the G3 hairpin was studied by Square Wave Voltammetry on a gold microelectrode array (Fig. 4a). Thiolated A3* was immobilized on the gold electrode, followed by backfilling with 6-mercaptohexanol (6MCH). G3 was then added to the electrode in a solution containing 50 µM of Methylene Blue (MB) (Fig. 4b). MB binds to single-stranded DNA regions by electrostatic interactions,

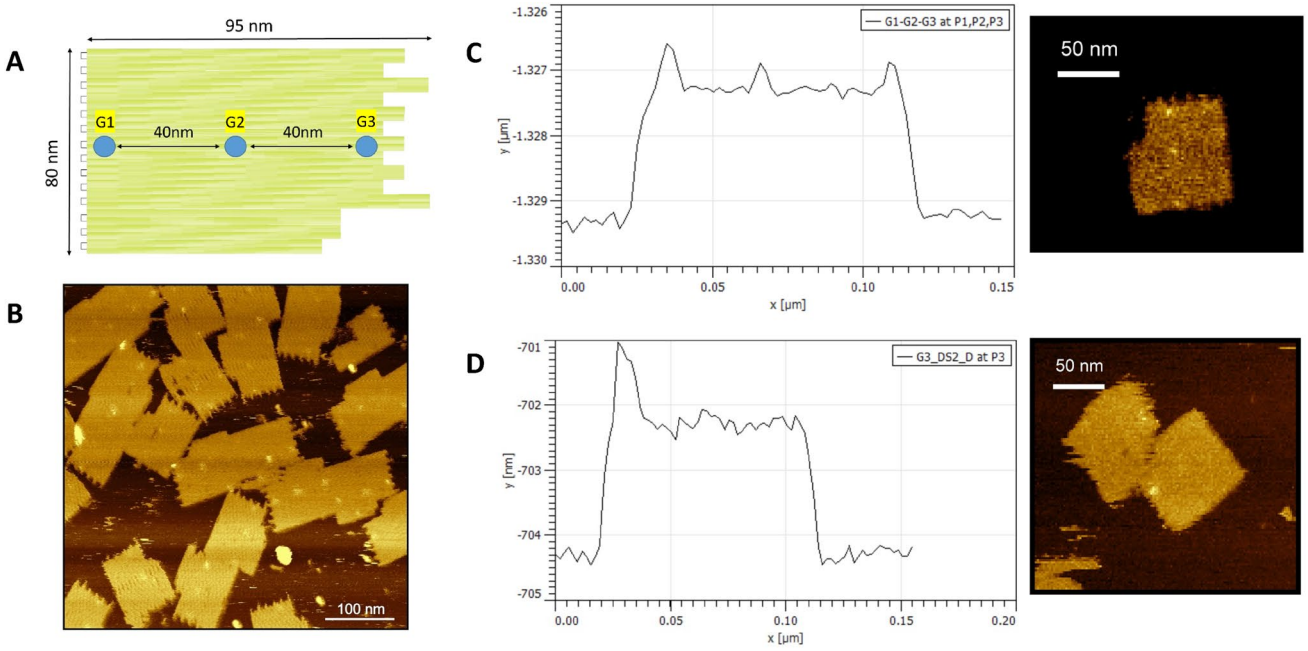

Fig. 2 **a** Schematic representation of the DNA origami structure and the location of hairpins G1, G2, G3. **b** Atomic force microscopy image of the DNA origami structure functionalized with hairpins G1–G3. **c** Line profile of the DNA origami with immobilised hairpins G1–G2–G3. **d** Line profile of DNA origami with immobilised hairpin G3

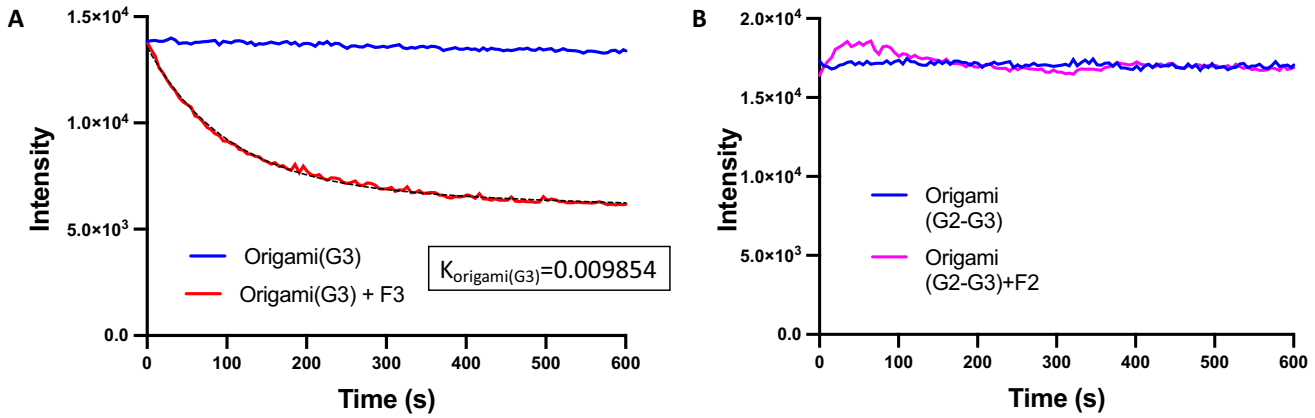

Fig. 3 **a** Hairpin opening kinetics of 1 nM of DNA origami functionalized with G3 with 2 nM final concentration of F3. **b** Hairpin opening kinetics of 1 nM of DNA origami functionalized with G2 + G3 with 2 nM final concentration of F2

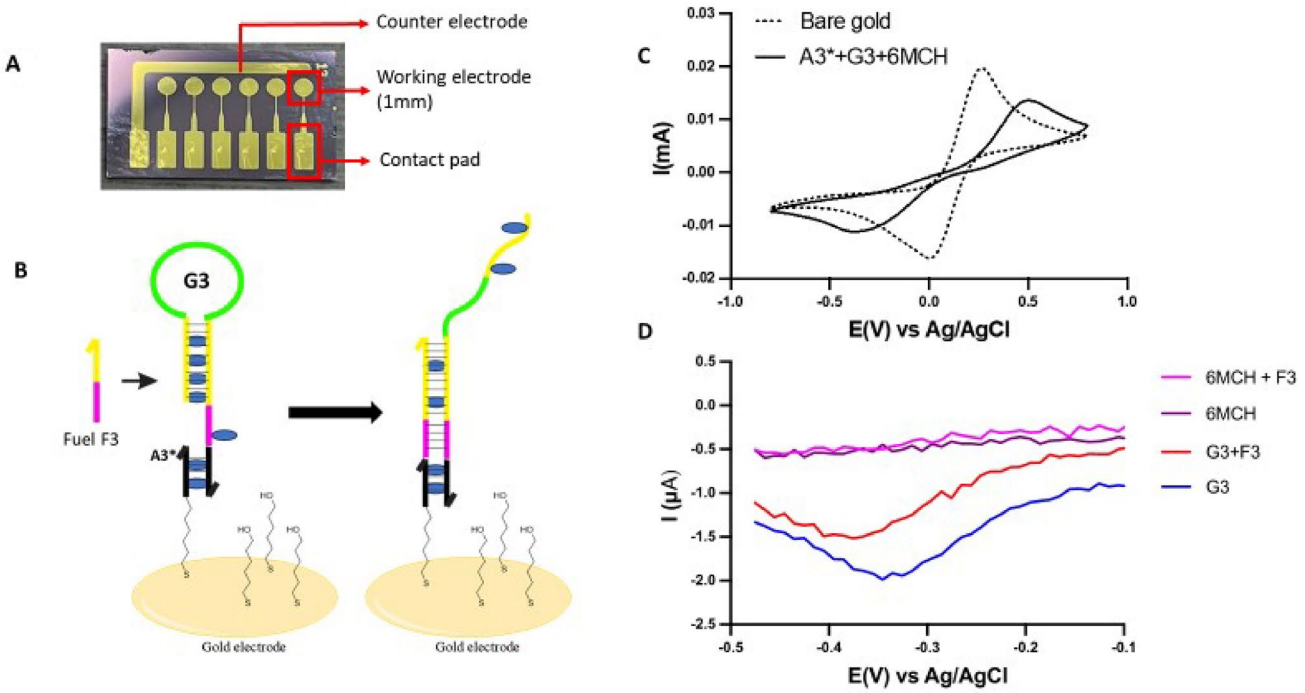

Fig. 4 **a** Gold microelectrode array used for electrochemical analysis. **b** Schematic representation of the molecular layer generated on the electrode surface. Methylene blue indicated by blue dots is either intercalated into the double strand or linked to the single stranded regions. **c** Cyclic Voltammetry of 9 mM of Potassium Ferro/ferricyanide (1:1) of bare and modified electrodes. **d** Square wave Voltammetry of modified electrodes either with just 1 μM 6MCH or 1 μM 6MCH + 1 μM G3, before and after incubating with 3 μM of F3

and to the double-stranded regions via π–π stacking [12]. The presence of the molecular layer was confirmed via the peak-to-peak distance of the cyclic voltammogram of 9 mM of potassium ferro/ferricyanide (1:1), which increased from 300 mV on the bare gold to 920 mV, proving the formation of a layer on top of the gold surface.

The principle of monitoring the opening of G3 electrochemically is based on the loss of methylene blue (MB) bound to the double-stranded regions of the closed hairpin upon opening of the hairpin. Electron transfer is therefore reduced. We can measure the reduction of MB by SWV applying an overpotential from − 0.1 to − 0.5 V. No signal was observed for 6MCH-modified electrodes with or without fuel F3, indicating nor MB or free hairpin is trapped in the molecular layer or adsorbed to the surface. Electrodes functionalized with the G3 yielded a cathodic current of ~ 1 μA.

When fuel F3 was added, the cathodic current decreased to ~ 0.5 µA. This promising, yet preliminary, results indicate the feasibility of measuring a cascade reaction by electrochemical means.

Discussion

We have shown some promising steps towards the development of an e-RADM. Single hairpin opening kinetics has been observed on very short timescales, and a hairpin-based cascade reaction was demonstrated in solution. We have also shown the successful immobilization of 3 different hairpins onto DNA origami and have been able to monitor the opening of such immobilized hairpins. Our preliminary results suggest that the opening of a single hairpin on the origami structure is slower compared to in solution. We speculate this could be the result of the reduced degrees of freedom of the hairpin immobilized on the origami structure. However, the difference in local concentration is also likely to play a role. This is difficult to normalize as we cannot determine the final hairpin concentration after the immobilization.

While no cascade reaction was observed on the origami structure, this was expected as the length of G2 when fully opened is smaller than 40 nm, the spacing with which the hairpins were positions. However, we note that further analysis of the system is required.

In conclusion, our preliminary electrochemical studies helped to expand our knowledge on the hairpin immobilization on the gold microelectrodes, as well as establish a procedure to analyse the opening of the hairpin by electrochemical means.

Supplementary Information The online version contains supplementary material available at https://doi.org/10.1557/s43580-024-00784-6.

Acknowledgments MAJM is grateful for the PhD scholarship from the University of Leeds.

Author contributions Prof. CW and Dr CW conceived and guided the project and provided critical feedback on all results. Mr. MAJ constructed and performed all experiments, analysed the data, and, with Prof. CW, prepared the manuscript.

Funding This work was funded by the University of Leeds.

Data availability The data associated with this paper are openly available from the University of Leeds Data Repository https://doi.org/10.5518/1509.

Declarations

Conflict of interest The authors declare that they have no conflict of interest.

References

1. P. Stanley, L. Strittmatter, A. Vickers, K. Lee, Biotechnol. Adv. (2020). https://doi.org/10.1016/j.biotechadv.2020.107639
2. J. Yoon, M. Mohammadniaei, H.K. Choi, M. Shin, B.G. Bharate, T. Lee, J.W. Choi, Appl. Surf. Sci. (2019). https://doi.org/10.1016/j.apsusc.2019.01.229
3. B. Sun, D. Liang, X. Li, P. Chen, J. Mater. Sci. Mater. Electron. (2015). https://doi.org/10.1007/s10854-015-4248-9
4. J. Xu, X. Zhao, X. Zhao, Z. Wang, Q. Tang, H. Xu, Y. Liu, Small Science (2022). https://doi.org/10.1002/smsc.202200028
5. Y. Dong, F. Sun, Z. Ping, Q. Ouyang, L. Qian, Natl. Sci. Rev. (2020). https://doi.org/10.1093/nsr/nwaa007
6. Y. Hao, Q. Li, C. Fan, F. Wang, Small Struct. (2020). https://doi.org/10.1002/sstr.202000046
7. D. Carmean, L. Ceze, G. Seelig, K. Stewart, K. Strauss, M. Willsey, Proc. IEEE (2019). https://doi.org/10.1109/JPROC.2018.2875386
8. L. Organick, S.D. Ang, Y.J. Chen, R. Lopez, S. Yekhanin, K. Makarychev, M.Z. Racz et al., Nat. Biotechnol. (2018). https://doi.org/10.1038/nbt.4079
9. A. Chen, B. Shah, Anal. Methods (2013). https://doi.org/10.1039/c3ay40155c
10. C. Xu, B. Ma, Z. Gao, X. Dong, C. Zhao, H. Liu, Sci. Adv. (2021). https://doi.org/10.1126/sciadv.abk0100
11. J.N. Zadeh, C.D. Steenberg, J.S. Bois, B.R. Wolfe, M.B. Pierce, A.R. Khan, R.M. Dirks, N.A. Pierce, J. Comput. Chem. (2011). https://doi.org/10.1002/jcc.21596
12. D. Yun, B. Chakraborty, B. Ge, H.Z. Yu, J. Phys. Chem. B (2012). https://doi.org/10.1021/jp302988t